

# On the Response of Neurons to Sinusoidal Current Stimuli: Phase Response Curves and Phase-Locking

Michael J. Schaus and Jeff Moehlis

**Abstract**—A powerful technique for analyzing mathematical models for biological oscillators is to reduce them to phase models, with a single variable describing the phase of the oscillation with respect to some reference state. From this reduction, one obtains the oscillator’s phase response curve (PRC), which determines its response to weak stimuli. In this paper, we show how properties of the PRC determine the parameter regimes for which the response of an oscillator is phase-locked to a sinusoidal stimulus. Furthermore, we show how knowledge of an oscillator’s phase-locking behavior can be used to deduce useful properties of the PRC. Our focus is on neural oscillators described by conductance-based models and stimulated by a sinusoidal current, although the results are expected to be relevant to other biological oscillators.

## I. INTRODUCTION

There are many natural and technological systems which undergo oscillations in mechanical, electrical, and/or chemical properties. Biological systems undergoing such oscillations include pacemaker cells in the heart [1] and the electrical activity of neurons [2]. A powerful technique for analyzing mathematical models for such oscillators is to reduce them to phase models, with a single variable describing the phase of the oscillation with respect to some reference state [3], [4], [5], [6]. From this reduction, one obtains the oscillator’s phase response curve (PRC), which ultimately determines its response to *any* weak stimulus (e.g. [7], [8]).

Our focus will be on the response properties of individual neurons to sinusoidal currents. This is a crucial step in the future study of the dynamics of *populations* of neurons subjected to periodic current stimuli along the lines of [7], [9], [10], work expected to be important for helping to provide a mathematical basis for the treatment of neurological disorders such as Parkinson’s disease using an FDA-approved therapeutic technique known as deep brain stimulation [11], [12], [10], [13]. Here a neurosurgeon guides a small electrode into the motor-control region of a patient’s brain, and then connects the electrode to a pacemaker implanted in the patient’s chest which sends high-frequency ( $> 100$  Hz) electrical pulses directly into the brain tissue in an attempt to control pathologically synchronized neural activity.

Specifically, in this paper we will determine the relationship between PRCs and phase-locking behavior of neurons, in which the stimulus frequency is an integer multiple of the response frequency. If the PRC is known, this allows for

very accurate predictions of the locations of phase-locking boundaries in parameter space. One can thus predict whether a neuron will phase-lock to a stimulus based on how close the stimulus frequency is to a multiple of the neuron’s natural frequency and how strong the stimulus is. If the PRC is not known, data points from the boundaries of phase-locking regions can be fit to give useful properties of the PRC, namely its Fourier content. This provides constraints on the procedures described in [14], [15] for deducing PRCs from noisy data.

Although our focus is on neural systems, it is expected that the results can also be applied to the study of circadian rhythms. Humans have a natural sleep-wake cycle slightly different from 24 hours, but due to the light-dark cycles of the sun, we are entrained to be on a 24-hour cycle. The techniques in this paper could help to clarify the properties of this entrainment and the PRC for circadian rhythms.

## II. PHASE EQUATIONS FOR NONLINEAR OSCILLATORS

### A. Phase reduction

Nonlinear oscillators with attracting limit cycles can have the limit cycle mapped to phase coordinates to simplify further analysis [3], [4], [5], [6], [7]. Here we consider a nonlinear oscillator described by a generic conductance-based model of a single neuron,

$$C\dot{V} = I_g(V, \vec{n}) + I_b + I(t), \quad (1)$$

$$\dot{\vec{n}} = \vec{N}(V, \vec{n}). \quad (2)$$

$V$  is the voltage across the membrane of the neuron,  $\vec{n}$  is the  $(N-1)$ -dimension vector of gating variables, and  $C$  is the membrane capacitance.  $I_g(V, \vec{n})$  is the vector of membrane currents,  $I_b$  is the baseline current that sets the natural frequency of the oscillator, and  $I(t)$  is a current stimulus. Examples of such models include the Hodgkin-Huxley equations (hereafter HH) [2] and the Hindmarsh-Rose equations (hereafter HR) [16]. It will prove useful to rewrite Equations (1) and (2) in the general form

$$\frac{d\vec{X}}{dt} = \vec{F}(\vec{X}), \quad (3)$$

where  $\vec{X} = (V, \vec{n})^T \in \mathbb{R}^N$  and  $\vec{F}(\vec{X})$  is the baseline vector field. We suppose that this system has an attracting limit cycle  $\vec{X}_0(t)$  with period  $2\pi/\omega$ .

We introduce the scalar phase variable  $\theta(\vec{X}) \in [0, 2\pi)$  for all  $\vec{X}$  in  $\mathcal{U}$ , some neighborhood of  $\vec{X}_0$  contained within its

This work was supported by a Sloan Research Fellowship in Mathematics and National Science Foundation grant NSF-0547606.

M.J. Schaus and J. Moehlis are with the Department of Mechanical Engineering, University of California, Santa Barbara, CA, 93117, USA moehlis@engineering.ucsb.edu

basin of attraction, such that the evolution of the phase takes the form

$$\frac{d\theta(\vec{X})}{dt} = \omega \quad (4)$$

for all  $\vec{X} \in \mathcal{U}$ . That is,  $\theta$  evolves linearly in time. This is accomplished by defining the level sets of  $\theta(\vec{X})$ , called *isochrons* [17], as follows. Let  $\vec{X}_0^S$  be the point on the limit cycle with the highest voltage, i.e. where the neuron spikes. We define  $\theta(\vec{X}_0^S) = 0$ . To determine  $\theta$  for another point on the limit cycle, say  $\vec{X}_0^P$ , one finds the time  $t$  for the system to evolve from  $\vec{X}_0^S$  to  $\vec{X}_0^P$ , and defines  $\theta(\vec{X}_0^P) = \omega t$ . This method assigns a value of  $\theta$  in  $[0, 2\pi)$  to every point on  $\vec{X}_0$ . The isochron associated with a point  $\vec{X}_0^P$  on  $\vec{X}_0$  is defined as the set of all initial conditions,  $\vec{X} \in \mathcal{U}$ , such that the distance (evaluated at time  $t$ ) between trajectories starting at  $\vec{X}_0^P$  and  $\vec{X}$  goes to zero as  $t \rightarrow \infty$ . The point  $\vec{X}_0^P$  and the points on its isochron,  $\vec{X}_{iso}^P$ , are said to have the same asymptotic phase.

Now, consider the system

$$\frac{d\vec{X}}{dt} = \vec{F}(\vec{X}) + \epsilon \vec{G}(\vec{X}, t), \quad (5)$$

where  $\epsilon$  is small, so that  $\epsilon \vec{G}(\vec{X}, t)$  is a small perturbation to the system. Using the chain rule and Equation (4) which tells us that  $d\theta/dt = \omega$  in the absence of perturbations,

$$\begin{aligned} \frac{d\theta}{dt} &= \frac{\partial \theta}{\partial \vec{X}} \cdot \frac{d\vec{X}}{dt} = \frac{\partial \theta}{\partial \vec{X}} \cdot (\vec{F}(\vec{X}) + \epsilon \vec{G}(\vec{X}, t)) \\ &= \omega + \epsilon \frac{\partial \theta}{\partial \vec{X}} \cdot \vec{G}(\vec{X}, t). \end{aligned} \quad (6)$$

Defining the *phase response curve* (PRC) as

$$\vec{Z}(\theta) = \left. \frac{\partial \theta}{\partial \vec{X}} \right|_{\vec{X}_0(\theta)}, \quad (7)$$

an approximation to Equation (6) is given by

$$\frac{d\theta}{dt} = \omega + \vec{Z}(\theta) \cdot \epsilon \vec{G}(\vec{X}_0, t). \quad (8)$$

Suppose now that the neuron is subjected to a current stimulus  $I(t)$ , which directly affects only the voltage of the neuron so that  $\epsilon \vec{G} = \epsilon \vec{G}(t) = (I(t), \vec{0})$ . Including  $C$  so that the units work out correctly and using only the voltage component of  $\vec{Z}(\theta)$ , the phase reduced equation for the neural oscillator becomes

$$\frac{d\theta}{dt} = \omega + \frac{Z(\theta)}{C} I(t). \quad (9)$$

The PRC can be written as

$$Z(\theta) = CZ_d \zeta(\theta), \quad (10)$$

where  $Z_d$  is a dimensional constant (units of *rad/coulomb*), and  $\zeta(\theta)$  is a nondimensional  $O(1)$  function. For this paper, the injected current is sinusoidal with the form

$$I(t) = I_f \sin(\omega_f t), \quad (11)$$

where  $I_f$  is the strength of the injected current in milliamperes and  $\omega_f$  is the angular frequency.

## B. Phase response curves

The PRC of a system determines how small perturbations in a given variable affect the system's phase. For neural oscillators such as in this paper, a useful way to think about the PRC is

$$Z(\theta) = \frac{\partial \theta}{\partial V} = \lim_{\Delta V \rightarrow 0} \frac{\Delta \theta}{\Delta V}, \quad (12)$$

with units *rad/mV*. To measure the PRC of a neuron, experiments can be done to measure  $\Delta\theta/\Delta V$  directly by injecting an impulse at a given phase and seeing how this impulse affects the arrival of the next spike. However, such experiments can be difficult to set up and often result in data with too much noise to be very useful.

## C. Phase-locking behavior

Regions of parameter space where phase-locking occurs are called Arnold tongues [18], [19]. Inside these tongues, forcing cycles and resulting forced oscillations have frequencies in specific ratios. In general,  $n : m$  phase-locking refers to  $n$  cycles of forcing resulting in  $m$  cycles of system oscillation. It is also useful to define the ratio  $\rho = m/n$ , called the rotation number [18]. When the system is outside of the Arnold tongues, phase-locking does not occur, corresponding to an irrational rotation number. In theory,  $n : m$  tongues exist for all  $n, m \in \mathbb{N}$ , but in real systems the vast majority have widths too small to measure [19].

## III. DEDUCING PHASE-LOCKING REGIONS FROM PHASE RESPONSE CURVES

In this section, it is assumed that the PRC  $Z(\theta)$  is known. This could be from the proximity of the neural system to a bifurcation which gives rise to its periodicity [7], from the numerical solution to the adjoint equations for the neural model of interest [7], [20], or from recently proposed least-squares fitting procedures which can be applied to experimental data [14], [15]. We will show how such knowledge of  $Z(\theta)$  can be used to find analytical approximations for the boundaries of phase-locked regimes.

Let  $\tau = \omega_f t$  be the nondimensionalized time. Equation (9) then becomes

$$\frac{d\theta}{d\tau} = \frac{1}{\lambda} + \mu \zeta(\theta) \sin \tau, \quad (13)$$

where the nondimensional quantities

$$\lambda = \frac{\omega_f}{\omega}, \quad \mu = \frac{I_f Z_d}{\omega_f} \quad (14)$$

measure the ratio between the forcing and natural frequencies, and the strength of the forcing, respectively. The solution  $\theta(\tau)$  cannot be found explicitly from Equation (13) through standard ODE techniques such as separation of variables. However, through averaging the equation, a close approximation to the solution can be found. We now show that averaging also allows approximations of phase-locking boundaries to be found.

Consider the system forced with frequency  $\omega_f \approx \frac{q}{p}\omega$ , i.e.

$$\frac{\omega}{\omega_f} = \frac{p}{q} + \epsilon \Delta, \quad (15)$$

where  $p$  and  $q$  are relatively prime integers and  $\epsilon\Delta$  represents a small detuning with respect to the center of the  $q : p$  phase-locking region. The system is put into a rotating reference frame by letting

$$\gamma = \theta - \frac{p}{q}\tau, \quad (16)$$

where  $\gamma$  is the difference in phase angle between the original system and the forcing, adjusted for proximity to the  $q : p$  tongue. This transforms Equation (13) into

$$\frac{d\gamma}{d\tau} = \epsilon\Delta + \mu\zeta\left(\gamma + \frac{p}{q}\tau\right) \sin \tau. \quad (17)$$

We then define

$$\epsilon\tilde{I}_f = I_f, \quad \epsilon\kappa = \epsilon\frac{\tilde{I}_f Z_d}{\omega_f} = \mu, \quad (18)$$

where  $\tilde{I}_f$  is an  $\mathcal{O}(1)$  amount of current, and  $\epsilon\kappa$  measures the strength of the forcing. Note that  $\epsilon$ ,  $\Delta$ , and  $\kappa$  are dimensionless. These transform Equation (17) into

$$\frac{d\gamma}{d\tau} = \epsilon\left[\Delta + \kappa\zeta\left(\gamma + \frac{p}{q}\tau\right) \sin \tau\right]. \quad (19)$$

Using the averaging theorem (Theorem 4.1 of [21]) and introducing the averaged variable  $\bar{\gamma}$ ,

$$\begin{aligned} \frac{d\bar{\gamma}}{d\tau} &= \frac{\epsilon}{2\pi q} \int_0^{2\pi q} \left[ \Delta + \kappa\zeta\left(\bar{\gamma} + \frac{p}{q}\tau\right) \sin \tau \right] d\tau \\ &= \epsilon \left\{ \Delta + \frac{\kappa}{2\pi q} \int_0^{2\pi q} \left[ \zeta\left(\bar{\gamma} + \frac{p}{q}\tau\right) \sin \tau \right] d\tau \right\} \\ &\equiv \epsilon(\Delta + g(\bar{\gamma})). \end{aligned} \quad (20)$$

The averaging theorem states that solutions to Equation (20) remain within  $\mathcal{O}(\epsilon)$  of solutions to Equation (19) (i.e.  $\gamma = \bar{\gamma} + \mathcal{O}(\epsilon)$ ) for times of  $\mathcal{O}(1/\epsilon)$ . Furthermore, fixed points of Equation (20) (i.e. values of  $\bar{\gamma}$  where  $d\bar{\gamma}/d\tau = 0$ ) correspond to the periodic orbits of Equation (19). The integration period of  $2\pi q$  was chosen because it is the smallest common multiple of the periods in the integrand.

Computing  $g(\bar{\gamma})$  for anything but the most simple PRCs gets difficult very quickly. To alleviate this problem, the PRC can be expanded as a Fourier series,

$$\begin{aligned} \zeta\left(\bar{\gamma} + \frac{p}{q}\tau\right) &= \sum_{j=0}^{\infty} \left[ a_j \cos\left(j\bar{\gamma} + j\frac{p}{q}\tau\right) \right] \\ &\quad + \sum_{j=1}^{\infty} \left[ b_j \sin\left(j\bar{\gamma} + j\frac{p}{q}\tau\right) \right]. \end{aligned} \quad (21)$$

The relationship between the coefficients in this series, e.g.  $a_j$ , and coefficients derived from the original PRC (with units  $rad/mV$ ), e.g.  $a_j^{PRC}$ , is

$$a_j = \frac{a_j^{PRC}}{CZ_d}, \quad (22)$$

which comes from Equation (10). For the terms in the series to contribute a non-zero value to  $g(\bar{\gamma})$  the sin term and the  $\zeta$  term must have the same frequency. Thus, we must have  $j\frac{p}{q} = 1$ . Since  $j = \frac{q}{p}$  must be an integer, this method of

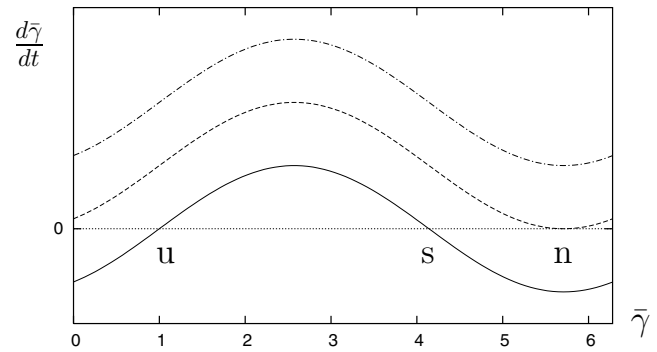


Fig. 1. Plot of the righthand side of (24) for different values of the detuning  $\Delta$ . The solid line is for small  $|\Delta|$ , and corresponds to a system with a stable (s) and unstable (u) periodic orbit. The dot-dashed line is for large  $|\Delta|$ , and corresponds to a system with no periodic orbits. The dashed line is for the critical value of  $|\Delta|$  which gives a neutrally stable periodic orbit (n).

averaging only gives nontrivial results for  $n : 1$  tongues. For other tongues, a higher-order averaging technique might provide better results. Taking this into account,  $g(\bar{\gamma})$  can be written as

$$g(\bar{\gamma}) = \frac{\kappa}{2\pi q} \int_0^{2\pi q} \left[ a_{q/p} \cos\left(\frac{q}{p}\bar{\gamma} + \tau\right) \sin \tau + b_{q/p} \sin\left(\frac{q}{p}\bar{\gamma} + \tau\right) \sin \tau \right] d\tau,$$

which evaluates to

$$g(\bar{\gamma}) = \frac{\kappa}{2} \left[ -a_{q/p} \sin\left(\frac{q}{p}\bar{\gamma}\right) + b_{q/p} \cos\left(\frac{q}{p}\bar{\gamma}\right) \right]. \quad (23)$$

Combining the sin and cos terms from Equation (23) to a single sin term with a phase lag turns Equation (20) into

$$\frac{d\bar{\gamma}}{d\tau} = \epsilon\Delta + \frac{\epsilon\kappa}{2} \sqrt{a_{q/p}^2 + b_{q/p}^2} \sin\left(\frac{q}{p}\bar{\gamma} - \tan^{-1} \frac{b_{q/p}}{a_{q/p}}\right). \quad (24)$$

Figure 1 shows the righthand side of (24) for different values of the detuning  $\Delta$ . For small  $|\Delta|$ , this intersects the line  $d\bar{\gamma}/d\tau = 0$  in two places, corresponding to one stable and one unstable periodic orbit. For large  $|\Delta|$ , it does not intersect  $d\bar{\gamma}/d\tau = 0$ , so that no periodic orbits exist. At the critical value of  $|\Delta|$ , it is tangent to  $d\bar{\gamma}/d\tau = 0$  at one point, corresponding to a neutrally stable periodic orbit, and the boundary of the  $q : p$  tongue. This occurs when

$$|\Delta| = \frac{\kappa}{2} \sqrt{a_{q/p}^2 + b_{q/p}^2}, \quad (25)$$

which is equivalent to

$$\left(\frac{1}{\lambda} - \frac{p}{q}\right) = \pm \frac{\mu}{2} \sqrt{a_{q/p}^2 + b_{q/p}^2}. \quad (26)$$

Rewriting with dimensional terms,

$$\left(\frac{\omega}{\omega_f} - \frac{p}{q}\right) = \pm \frac{I_f}{2\omega_f C} \sqrt{(a_{q/p}^{PRC})^2 + (b_{q/p}^{PRC})^2}. \quad (27)$$

Figure 2 shows the averaged solution to the whole-number ratio phase-locking regions of the HH system with standard

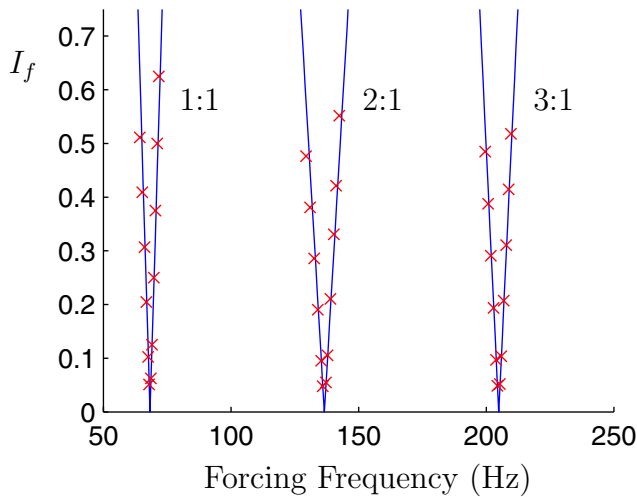


Fig. 2. The lines show predicted phase-locking boundaries for the HH system with standard parameters and baseline current  $I_b = 10$ . The points here and in other plots come from numerically finding the boundaries through a frequency sweep method, such as what an experimentalist might use (see [22]).

parameters and baseline current  $I_b = 10$  [2]. Also included are points from these boundaries found numerically from integration of the full HH system with a sinusoidal current stimulus (see [22]). The plot confirms that by knowing the PRC of a system, the phase-locking regions can be very accurately predicted.

#### IV. USING PHASE-LOCKING DATA TO DEDUCE PROPERTIES OF THE PHASE RESPONSE CURVE

In this section, we assume that the PRC  $Z(\theta)$  is *not* known for the system of interest. We show how data points on the phase-locking boundaries can be used to deduce useful properties of the PRC. We separate our discussion into two classes of neurons [23]: Type I, slow neurons which tend to fire at  $\mathcal{O}(1)$  frequencies, and Type II, fast neurons which tend to fire with  $\mathcal{O}(10)$  frequencies. The distinction between Type I and Type II neurons can be related to the bifurcation which leads to periodic firing, which allows one to deduce approximate analytical expressions for their PRCs (e.g. [7]).

##### A. Type I Neurons

Figure 3 shows data for the 1:1 phase-locking boundary for the HR system, a two-dimensional set of equations giving prototypical Type I behavior [16]. Data was taken for three different values of the baseline current ( $I_b = 4.95, 5.00, 5.10$ ), corresponding to three different natural frequencies.

Normal form calculations predict that PRCs for Type I neurons take the form [23], [7]

$$Z(\theta) = \frac{c_{sn}}{\omega} (1 - \cos \theta), \quad (28)$$

where  $c_{sn}$  is a constant. The approximate phase-locking boundary for this PRC found from (27) is then

$$\frac{\omega}{\omega_f} - 1 = \pm \frac{I_f c_{sn}}{2\omega\omega_f C}. \quad (29)$$

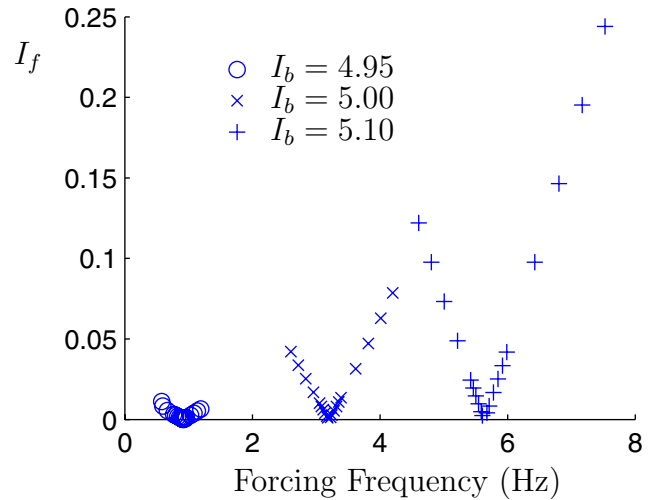


Fig. 3. Raw data taken for the 1:1 phase-locking boundary of the HR system for three values of  $I_b$ .

Solving for  $I_f$  as a function of  $\omega_f$ ,

$$I_f = \mp \frac{2\omega C}{c_{sn}} (\omega - \omega_f). \quad (30)$$

Letting

$$\beta = \frac{I_f}{2\omega\omega_f C}, \quad (31)$$

Equation (30) becomes

$$\beta = \frac{1}{c_{sn}} \left( \frac{1}{\lambda} - 1 \right). \quad (32)$$

Fitting an appropriate subset of the data from Figure 3 to Equation (32) yields the value  $c_{sn} = 0.00358$ , with the corresponding PRC compared with actual PRCs in Figure 4. These results show that this method captures the general shape as well as the magnitude of the PRC with less than 6% error. We note that both  $\lambda$  and  $\beta$  can be readily computed from experimental data.

##### B. Type II Neurons

The top panel of Figure 5 shows data for the 1:1 phase-locking boundary for HH neurons, which are of Type II. Data was taken for three different values of the baseline current ( $I_b = 6.6, 10.0, 20.0$ ), corresponding to three different natural frequencies.

It has been proposed that the PRCs for Type II neurons can be approximated as

$$Z(\theta) = \frac{|c_B|}{|\omega - \omega_{SN}|} \sin(\theta - \phi_B), \quad (33)$$

where  $c_B, \omega_{SN}$ , and  $\phi_B$  are constants [7]. The approximate phase-locking boundary for this PRC found from (27) is then

$$\frac{\omega}{\omega_f} = 1 \pm \frac{I_f |c_B|}{2\omega_f |\omega - \omega_{SN}| C}. \quad (34)$$

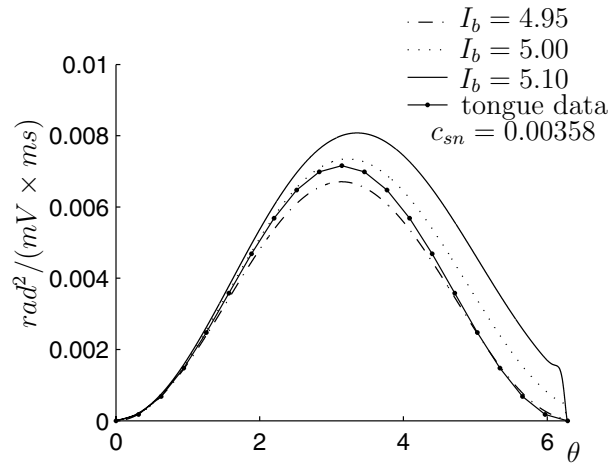


Fig. 4. Comparison of actual PRCs and the PRC from (28) with  $c_{sn}$  obtained by fitting the tongue data from Figure 3. All curves are multiplied by  $\omega$  to remove the expected  $\omega$  dependence of the magnitude of the PRCs [7].

Using  $\lambda$  and  $\beta$  as above in Equation (34) gives

$$\beta = \frac{|\omega - \omega_{SN}|}{\omega |c_B|} \left( \frac{1}{\lambda} - 1 \right). \quad (35)$$

We used the data from the top panel of Figure 5 in (35) to obtain the best fit values for  $\omega_{SN}$  and  $c_B$ ; the bottom panel of Figure 5 compares the corresponding tongue to the tongues from the top panel, plotted using nondimensionalized variables. Table I compares the actual and predicted values of the Fourier content of the PRC. The predicted values come from the amplitude of (33) for the fitted values of  $\omega_{SN}$  and  $c_B$ . This shows that the 1:1 phase-locking tongue can be used to accurately predict the combination of the first terms in the Fourier decomposition of the PRC.

One might suspect that using phase-locking data from the 2:1 and 3:1 tongues (and so on) would allow for a more accurate representation of the PRC to be put together, but this procedure only gives the quantity  $\sqrt{a_j^2 + b_j^2}$ , not the individual  $a_j$  and  $b_j$  values, meaning no phase information about the Fourier terms is available. However, knowing the quantity  $\sqrt{a_j^2 + b_j^2}$  does allow for constraints to be obtained for use with procedures to find PRCs from experimental data recently proposed in [14], [15]. These procedures use least-squares fits to individual Fourier terms, so knowing the relationships between some of the terms could lead to better results.

#### V. DEDUCING NEURON TYPE FROM PHASE-LOCKING DATA

Phase-locking data can also be used to determine if a neuron is Type I or Type II. This is accomplished by finding the best fit for the data using approximate phase-locking boundaries corresponding to the PRCs (28) and (33), and determining which one minimizes the variance of the fit while still suggesting parameters which are physically

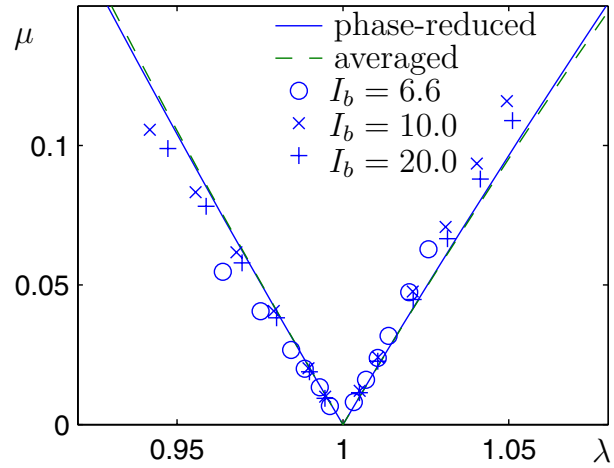
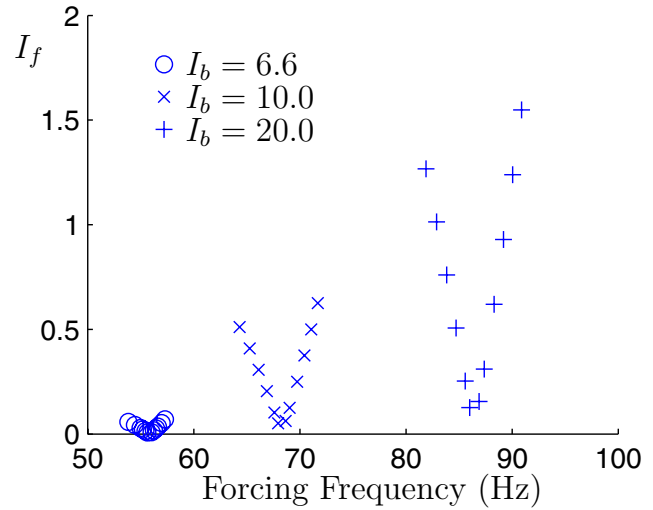


Fig. 5. Top panel: Raw data taken for phase-locking boundary of the HH system for three values of  $I_b$ . Bottom panel: Same data nondimensionalized using  $c_B$  and  $\omega_{SN}$  found from the fit described in the text. The solid line shows the numerically obtained boundary from (13), while the dashed line shows the predicted boundary from averaging.

TABLE I  
COMPARISON OF ACTUAL (SECOND COLUMN) AND PREDICTED (THIRD COLUMN) FOURIER CONTENT FOR THE HH SYSTEM FOR DIFFERENT VALUES OF  $I_b$ .

$I_b$	$\sqrt{(a_1^{PRC})^2 + (b_1^{PRC})^2}$	$\frac{ c_B }{ \omega - \omega_{SN} }$	% Error
6.6	0.320	0.322	0.6
10.0	0.0793	0.0835	5.4
20.0	0.0399	0.0402	0.7

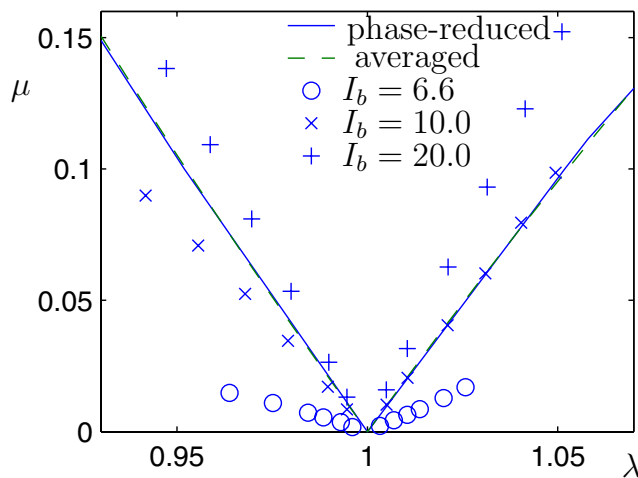


Fig. 6. Best fit of nondimensionalized data from top panel of Figure 5 to the nondimensionalized tongue expected for the Type I PRC given by (28).

allowed. As an illustration, suppose we did not know if the data shown in the top panel of Figure 5 corresponded to a Type I or a Type II neuron. Figure 6 shows the best fit of this data to the tongue expected for the Type I PRC given by (28). Clearly this is a much poorer fit than shown in the bottom panel of Figure 5. We can thus deduce that this data is better described as coming from a Type II rather than a Type I neuron. More detail on how one can deduce neuron type from phase-locking data is given in [22].

## VI. CONCLUSIONS AND FUTURE WORK

Neurons will phase-lock to a sinusoidal stimulus if their natural frequency is close enough to a rational multiple of the stimulus frequency and the stimulus is sufficiently strong. This paper has demonstrated the relationship between phase-locking regions of parameter space and the phase response curve (PRC) of the neuron, which characterizes how a neuron responds to impulsive stimuli. Indeed, knowledge of the PRC can be used to generate good predictions for the whole-number ratio phase-locking tongue boundaries, and the phase-locking tongues can be used to get useful information about the PRC. In the case of Type I neurons, data from the 1:1 tongue can lead to a very good approximation of the PRC. For Type II neurons, data from the tongues can be used to find combinations of the Fourier coefficients of the PRC which can be used as constraints in fitting procedures that generate Fourier coefficients of the PRC from experimental data [14], [15].

This work represents a crucial step in the future study of the dynamics of *populations* of oscillators subjected to sinusoidal forcing. Of particular interest is how quickly a group of oscillators can be synchronized or desynchronized and if there are any special distributions the neurons take, work which is expected to be important for helping to provide a theoretical basis for the treatment of neurological disorders such as Parkinson's disease using the FDA-approved therapeutic technique known as deep brain stimulation. Such

work will also consider the effects of coupling, noise, and distributions of the individual neuron's natural frequencies on the response properties of the population.

## REFERENCES

- [1] D. C. Michaels, E. P. Matyas, J. Jalife, Mechanisms of sinoatrial pacemaker synchronization - a new hypothesis, *Circ. Res.* 61 (1987) 704–714.
- [2] A. L. Hodgkin, A. F. Huxley, A quantitative description of membrane current and its application to conduction and excitation in nerve, *J. Physiol.* 117 (1952) 500–544.
- [3] A. Winfree, Patterns of phase compromise in biological cycles, *J. Math. Biol.* 1 (1974) 73–95.
- [4] J. Guckenheimer, Isochrons and phaseless sets, *J. Math. Biol.* 1 (1975) 259–273.
- [5] Y. Kuramoto, *Chemical Oscillations, Waves, and Turbulence*, Springer, Berlin, 1984.
- [6] A. Winfree, *The Geometry of Biological Time*, Second Edition, Springer, New York, 2001.
- [7] E. Brown, J. Moehlis, P. Holmes, On the phase reduction and response dynamics of neural oscillator populations, *Neural Comp.* 16 (2004) 673–715.
- [8] B. S. Gutkin, G. B. Ermentrout, A. D. Reyes, Phase response curves give the responses of neurons to transient inputs, *J. Neurophysiol.* 94 (2005) 1623–1635.
- [9] E. Brown, J. Moehlis, P. Holmes, E. Clayton, J. Rajkowski, G. Aston-Jones, The influence of spike rate and stimulus duration on noradrenergic neurons, *J. Comp. Neuroscience* 17 (2004) 13–29.
- [10] P. A. Tass, *Phase Resetting in Medicine and Biology*, Springer, New York, 1999.
- [11] A. L. Benabid, P. Pollak, C. Gervason, D. Hoffmann, D. M. Gao, M. Hommel, J. E. Perret, J. D. Rougemont, Long-term suppression of tremor by chronic stimulation of the ventral intermediate thalamic nucleus, *The Lancet* 337 (1991) 403–406.
- [12] S. Blond, D. Caparros-Lefebvre, F. Parker, R. Assaker, H. Petit, J.-D. Guieu, J.-L. Christiaens, Control of tremor and involuntary movement disorders by chronic stereotactic stimulation of the ventral intermediate thalamic nucleus, *J. Neurosurg.* 77 (1992) 62–68.
- [13] P. A. Tass, Synergetics of the nervous system: from basic principles to therapy, *Nonlin. Phenom. Complex Syst.* 5 (2002) 470–478.
- [14] R. F. Galan, G. B. Ermentrout, N. N. Urban, Efficient estimation of phase-resetting curves in real neurons and its significance for neural-network modeling, *Phys. Rev. Lett.* 94 (2005) 158101.
- [15] E. M. Izhikevich, *Dynamical Systems in Neuroscience: The Geometry of Excitability and Bursting*, Springer, New York, 2006, to be published.
- [16] R. Rose, D. Hindmarsh, The assembly of ionic currents in a thalamic neuron I. The three-dimensional model, *Proc. R. Soc. Lond. B* 237 (1989) 267–288.
- [17] K. Josic, E. T. Shea-Brown, J. Moehlis, Isochron, Scholarpedia, <http://www.scholarpedia.org>.
- [18] A. Pikovsky, M. Rosenblum, J. Kurths, *Synchronization: A Universal Concept in Nonlinear Sciences*, Cambridge University Press, Cambridge, 2001.
- [19] S. Wiggins, *Introduction to Applied Nonlinear Dynamical Systems and Chaos*, Second Edition, Springer, New York, 2003.
- [20] G. B. Ermentrout, *Simulating, Analyzing, and Animating Dynamical Systems: A Guide to XPPAUT for Researchers and Students*, SIAM, Philadelphia, 2002.
- [21] J. Guckenheimer, P. J. Holmes, *Nonlinear Oscillations, Dynamical Systems and Bifurcations of Vector Fields*, Springer-Verlag, New York, 1983.
- [22] M. Schaus, Neural oscillator identification via phase-locking behavior, Master's thesis, University of California, Santa Barbara (2005).
- [23] G. B. Ermentrout, Type I membranes, phase resetting curves, and synchrony, *Neural Comp.* 8 (1996) 979–1001.